ACADEMIC PRESS

Available online at www.sciencedirect.com

SCIENCE DIRECT®

Journal of Sound and Vibration 268 (2003) 751–778

JOURNAL OF SOUND AND VIBRATION

www.elsevier.com/locate/jsvi

Effects of isolators internal resonances on force transmissibility and radiated noise

Y. Du[a], R.A. Burdisso[a,*], E. Nikolaidis[b], D. Tiwari[b]

[a] *Vibration and Acoustics Laboratories, Department of Mechanical Engineering, Virginia Polytechnic Institute and State University, Blacksburg, VA 24061-0238, USA*

[b] *Mechanical, Industrial and Manufacturing Engineering Department, The University of Toledo, Toledo, OH 43606-3390, USA*

Received 15 October 2001; accepted 23 November 2002

Abstract

Vibration isolators have been extensively used to reduce the vibration and noise transmitted between the components of mechanical systems. Although some previous studies on vibration isolation considered the inertia of isolators, they only examined its effects on the vibration of single degree-of-freedom (d.o.f.) systems. These studies did not emphasize the importance of the isolators' inertia, especially from the perspective of noise reduction. This paper shows that the *internal dynamics* of the isolator, which are also known as *internal resonances* (IRs) or *wave effects*, can significantly affect the isolator performance at high frequencies. To study the IR problem, a model of a primary mass connected to a flexible foundation through three isolators is used. In this model, the isolator is represented as a one-dimensional continuous rod that accounts for its internal dynamics. The primary mass is modelled as a rigid body with three d.o.f.'s. The effects of the IRs on the force transmissibility and the radiated sound power from the foundation are examined. It is shown that the IRs significantly increase the force transmissibility and the noise radiation level at some frequencies. These effects cannot be predicted using a traditional model that neglects the inertia of the isolator. The influence of the foundation flexibility on the IRs is also investigated. It is shown that the foundation flexibility greatly affects the noise radiation level but it affects only slightly the force transmissibility, especially at high frequencies where the IRs occur.

*Corresponding author. Tel.: 540-231-4162; fax: 540-231-8836.
E-mail address: yudu@vt.edu, rburdiss@vt.edu (R.A. Burdisso).

0022-460X/03/$ - see front matter
doi:10.1016/S0022-460X(03)00036-1

1. Introduction

Vibration isolators have been extensively used to reduce the vibration induced in structures, e.g., automobiles, buildings, airplanes, and so forth, by machinery and to protect sensitive equipment from vibrations of the supporting structure.

A traditional vibration isolation model deals with a rigid mass, representing a piece of equipment, mounted on a rigid supporting structure via a massless isolator with pure spring stiffness and viscous damping as shown in Fig. 1(a). (The term *traditional* in this paper refers to a model with a massless isolator or a model with a massless isolator and viscous damping.) Normally, the primary mass is assumed to have only one degree of freedom (d.o.f.) that results in a single d.o.f. (s.d.o.f.) system. This model can be found in many textbooks and papers on mechanical vibrations [1–3].

The performance of an isolator is normally determined using the force transmissibility function, which is defined as the ratio of the transmitted force through the isolator to the excitation force. The force transmissibility curve of the traditional model with an ideal, i.e., massless, isolator has only one peak corresponding to the *system resonance* at the natural frequency ω_n. As shown in Fig. 2, the traditional model predicts that the attenuation of the transmissibility will occur at frequencies $\omega > \sqrt{2}\omega_n$. For a low damping ratio, e.g., $\zeta \leqslant 0.1$, and frequencies well above the

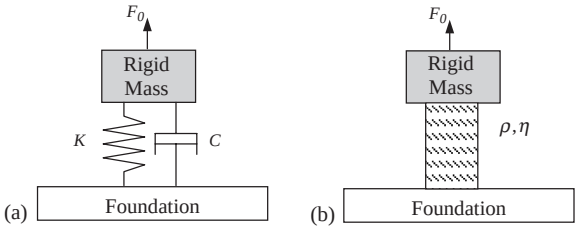

Fig. 1. Isolator modelled as (a) massless spring and a viscous damper or (b) continuous rod with mass, stiffness and damping.

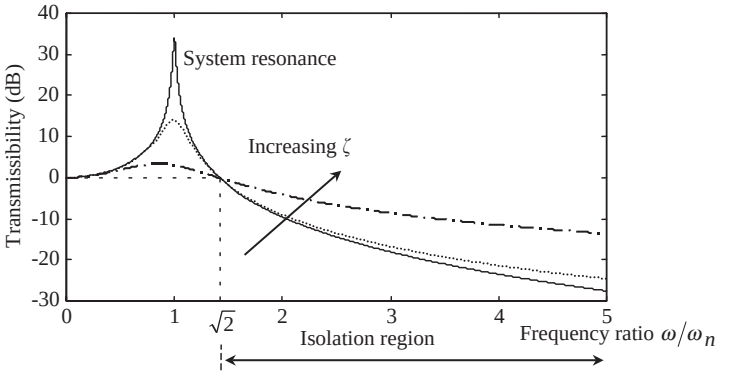

Fig. 2. The transmissibility function of the traditional s.d.o.f. model with massless isolator: ——, $\zeta = 0.01$; · · · · · · · · · · · ·, $\zeta = 0.1$; –·–·–, $\zeta = 0.5$.

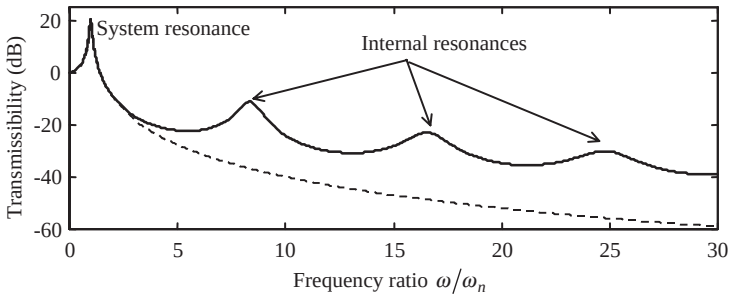

Fig. 3. Typical transmissibility function of realistic vibration isolator: – – – –, massless isolator; ——, realistic isolator.

system resonant frequency, the transmissibility decreases at a rate of 12 dB per octave [4, 5]. For frequencies $\omega < \sqrt{2}\omega_n$, the transmissibility is greater than one, i.e., the isolator amplifies the transmitted force. The transmissibility at the resonant frequency reduces, while the isolator performance degrades in the isolation region, as the damping ratio increases.

However, practical isolators have mass, and thus they have their own dynamics. These dynamics are associated with the resonance behavior of the elastic motion of the isolator, and they are known as the *internal resonances* (IRs) of isolators. Fig. 1(b) shows a more "realistic" isolator model than that of Fig. 1(a), which can illustrate the phenomenon of IRs. The isolator is modelled as a continuous elastic rod with density ρ and structural damping characterized by the loss factor η. The force transmissibility function of the s.o.d.f. system with this isolator model is plotted in Fig. 3. For comparison, the transmissibility of the same system calculated using the traditional model with the same damping is also shown in Fig. 3. Compared with the traditional massless model, the transmissibility curve of the "realistic" isolator shows peaks at the system resonance (as the massless isolator) as well as at the isolator's IRs. In addition, the transmissibility for the realistic isolator does not decrease monotonically with frequency, as it would for a massless isolator. So if one neglects the mass effects of a realistic isolator, one will over-estimate the performance of the isolator at high frequencies.

Since 1950s, several authors have studied isolators' IRs (also referred as *wave effects*) in both metal springs [6, 7] and viscoelastic isolators [4, 5, 8–11]. Since the lower the loss factor of the isolator the more significant are the wave effects, the IR problem in metal springs has attracted more attention than that in viscoelastic isolators because of the low damping of metal materials. Lee and Thompson [6] pointed out that the IRs in metal coil springs lead to significant dynamic stiffening above a certain frequency. For an automotive suspension spring, this occurs at frequencies as low as about 40 Hz. Lee and Thompson presented a method for calculating the dynamic stiffness of a helical coil spring and obtained the natural frequencies corresponding to the internal resonances from this method. Tomlinson [7] described the wave effects and demonstrated their importance in metal coil springs both theoretically and experimentally. Tomlinson also proposed a method to minimize the wave effects by using a parallel-mount isolator, which employs a metal coil spring acting in parallel with a polymeric damping material. The polymeric material, which has a high loss factor, helps dissipate the wave effects while the metal coil spring supports heavy components.

Most of the viscoelastic isolators are made of rubber materials. To the best of the authors' knowledge, the idealized "long-rod" model for a cylindrical rubber isolator was generally used by

previous researchers to show the wave effects. Ungar and Dietrich [8] calculated the IRs for some isolators that have simple geometries and deformation. They qualitatively explained that the wave effects are more important in a heavier, larger isolator than those in a lighter, smaller isolator of equal static stiffness. Harrison et al. [4] studied the wave effects in isolation mounts by evaluating the force transmissibility both analytically and experimentally. They concluded that the wave effects could increase the transmissibility of a mount in certain frequency ranges by as much as 20 dB above the transmissibility that would be predicted from the massless isolator theory. They also mentioned that for practical mounts, wave effects are most detrimental in the most audible frequency range (500–1000 Hz). The effects of the IRs change with the material properties of isolators. Sykes [9] tabulated data about the dynamic mechanical properties for some common mount materials, which permits one to estimate IRs from known wave velocities. These wave velocities are governed by properties of isolator material, as well as by the deformation type (e.g., shear, compression, flexure). Ungar [10] compared the wave effects in viscoelastic leaf (flexural waves) and compression (longitudinal waves) spring mounts. Snowdon [5,11] pointed out that the wave effects would be observed in high frequencies when the mount dimensions become comparable with multiples of the half-wavelengths of the elastic waves traveling through the mounting. Although Snowdon also noticed that the wave effects could impair the isolator's performance, he concluded that they are not always important because the relatively high damping in practical rubber isolators could attenuate these wave effects.

The majority of previous results were obtained using a simple s.d.o.f. model that accounts for the isolator's mass. This model only examines the IRs effects on the vibration isolation. However, the major limitation of previous studies is that they did not investigate the IR problem from the perspective of noise reduction. As mentioned earlier in this paper, although the IR problem has been identified, some researchers concluded that this problem is not significant. The authors believe that this conclusion can be wrong, and that the IRs can be important because: (1) previous studies examined the effects of IRs on the vibration but not on the radiated noise of a system; (2) IRs occur at high frequencies (e.g., above 500 Hz), where noise is particularly bothersome, and previous researchers did not investigate the isolator performance in this frequency range; and (3) previous researchers used a s.d.o.f. model, which is not adequate to investigate the significance of the IRs in practical isolators.

The objective of this paper is to study the effects of the IRs of vibration isolators on the isolator performance in terms of both vibration isolation and noise reduction. The effects of IRs and their significance will be shown by comparing the response of a system with ideal massless isolators to the response of the same system but with practical isolators that have mass.

In the following sections, an analytical model is first developed. This model uses three d.o.f.'s to describe the motion of the primary mass. Therefore, it represents a practical isolation system more accurately than a s.d.o.f. model. When modeling an isolator, this paper adopts the "long-rod" theory as used by previous researchers. The isolator has constant modulus and loss factor in the frequency range that is of interest, which is approximately true for most practical vibration isolators [4,5]. This treatment allows the model to show the importance of IRs without introducing additional complexity. In addition, the effect of the variation of the isolator's modulus and loss factor with frequency is also briefly discussed. The "slender rod" model is applicable to both cylindrical isolators made of viscoelastic materials and helical springs made of metallic materials because helical springs can be considered as long-rods in longitudinal vibration

[7]. The effects of the IRs on an isolator's performance are assessed using two metrics: (1) the force transmissibility of the isolator, and (2) the sound radiated by the foundation. Previous authors did not consider the second metric. It is shown that the IRs can increase the force transmissibility in certain frequency ranges by as much as 20–30 dB above the transmissibility predicted from a massless isolator model. The IRs can also increase the noise radiated by the foundation of a system with ideal, massless isolators by 3–22 dB in the frequency range from 200 to 3000 Hz.

2. Modelling approach for the internal resonance problem

This section describes the analytical model used to investigate the effects of isolators' IRs on the force transmissibility and the radiated noise. As shown in Fig. 4, the model is developed based on a system consisting of a primary mass connected to a flexible foundation through three isolators. The system is subjected to an external force with amplitude F_0 acting at an arbitrary location on the primary mass. This vibration system could be an idealization of an engine supported through three isolators to the body of a car. The primary mass is modeled as a rigid body with three d.o.f.s, which are the translation in the y- (vertical) direction and rotations about the x- and z- axis through the center of gravity. Therefore, the center of gravity of the primary mass can only move in the vertical direction. This model is called *3 d.o.f. model* based on the number of d.o.f. of the primary mass. To directly relate the motion of the primary mass with the displacements at the ends of the isolators, the three vertical translations, Y_{Ti}, where $i=1$, 2, and 3, at the mounting points between the isolators and the primary mass are used as the three d.o.f. s of the primary mass in the model. Each isolator is considered as a "one-dimensional" continuous rod that accounts for its own inertia. All joints between the isolators and the primary mass, and between the isolators and the foundation are pinned. Therefore, each isolator transfers forces along its axis only. The flexible foundation is considered as a simply supported rectangular plate that can vibrate and radiate noise to the ambient fluid. The displacements at the connection points between the isolators and the foundation are denoted as Y_{Bi}. Because the forces transmitted through the

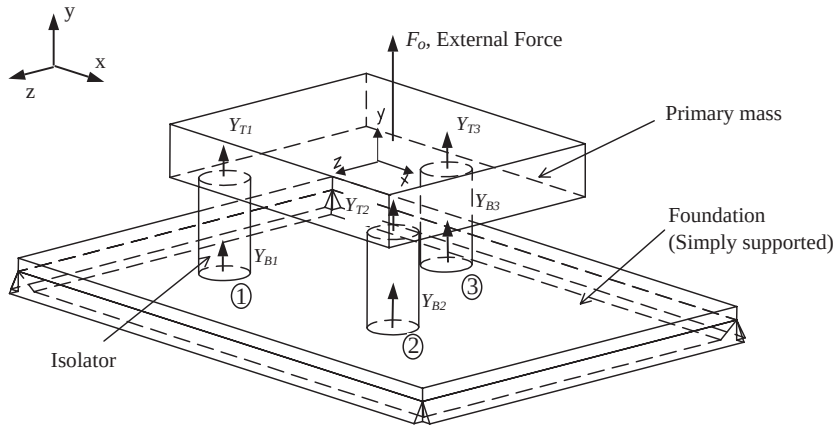

Fig. 4. A rigid primary mass with 3.d.o.f. connected to a flexible foundation through three isolators.

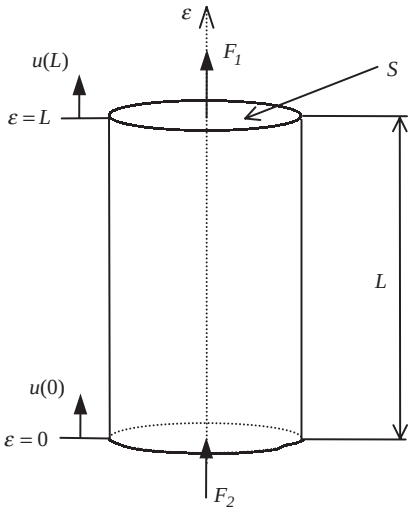

Fig. 5. Continuous model of the isolator.

isolators are considered as the only inputs to the plate, the radiated noise by the plate is sensitive to changes in the isolator performance. Furthermore, for the system considered in Fig. 4, only the noise radiated by the foundation is affected by the isolator's properties. Therefore, when examining the IR effects, only the acoustic power radiated by the foundation will be calculated.

The equations of motion (EOM) of the components and the system in Fig. 4 are presented in the following sections. The model is developed in the frequency domain so both the force transmissibility and the radiated sound power are given as functions of frequency.

2.1. Dynamic stiffness matrix of the isolator

Each of the cylindrical isolator in the 3d.o.f. system is modelled as a continuous uniform rod in axial motion as shown in Fig. 5. The relationship between the longitudinal displacements and external forces at the ends of the isolator is given by

$$[D]\begin{Bmatrix} u(L) \\ u(0) \end{Bmatrix} = \begin{Bmatrix} F_1 \\ F_2 \end{Bmatrix}, \tag{1}$$

where

$$[D] = \begin{bmatrix} D^d & -D^o \\ -D^o & D^d \end{bmatrix}, \tag{2}$$

is the dynamic stiffness matrix of the isolator. The terms in matrix $[D]$ are obtained in closed form in Appendix A. These terms are:

$$D^d = kS\tilde{E}\cot(kL), \quad D^o = \frac{kS\tilde{E}}{\sin(kL)}, \tag{3a, b}$$

where $\tilde{E} = E(1 + j\eta)$ is the complex modulus of elasticity; E is the modulus of elasticity, i.e., Young's modulus in this case; η is the loss factor; $k = \omega/c$ is the wavenumber; $c = \sqrt{\tilde{E}/\rho}$ is the complex wave speed in the isolator; ρ is the density, S is the isolator's cross-sectional area, and L is the length of the isolator.

2.2. Equilibrium equations of the system consisting of the primary mass, the isolators and the foundation

The EOM of the fully coupled system in Fig. 4 is derived by first modelling the substructures consisting of (a) the primary mass and isolators, and (b) the foundation separately. The two substructures are then coupled by imposing conditions for continuity of forces and displacements at their interfaces, i.e., at the isolators' attachment to the foundation. Fig. 6 shows the substructure consisting of the primary mass and the isolators separated from the foundation. Since only the displacement at each end of the isolators is of interest, six displacements need to be calculated. These are the six d.o.f.s used to describe the motion of the primary mass–isolators substructure. Displacements at the mounting points between the primary mass and isolators are denoted by subscript "T" (top of the isolator), while displacements at the mounting points between the foundation and isolators are denoted by subscript "B" (bottom of the isolator).

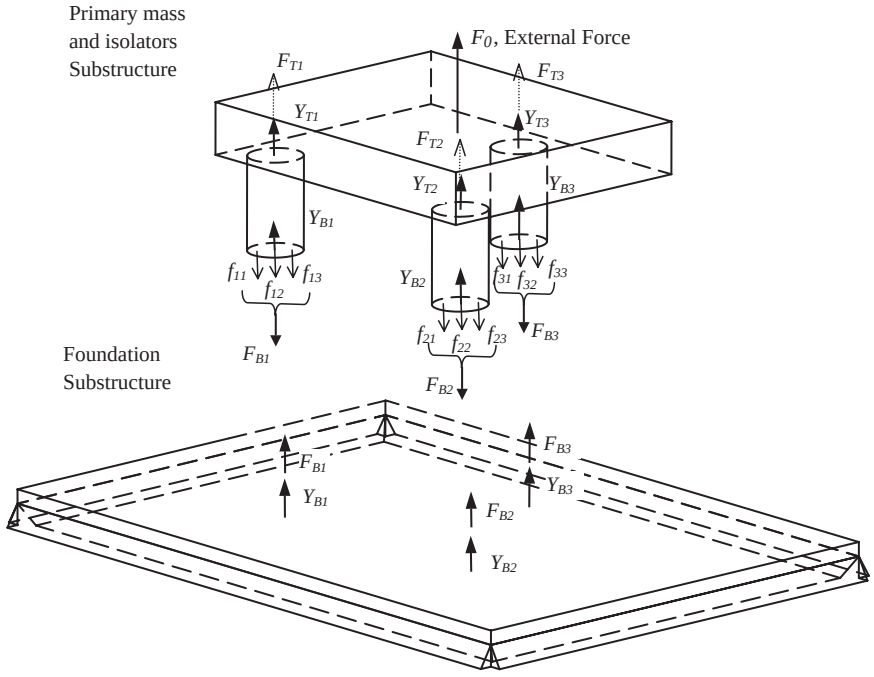

Fig. 6. Illustration for separating the primary mass and isolators from the foundation. (The external forces F_{T1}, F_{T2} and F_{T3} next to the dotted line are calculated from and are equivalent to the original external force F_0; f_{ij} denotes the transmitted force through isolator i due to the external force F_{Tj}.)

The EOMs of the primary mass–isolators substructure can be written as (see Appendix B for detail)

$$[D_s]\begin{Bmatrix} Y_{T_1} \\ Y_{T_2} \\ Y_{T_3} \\ Y_{B_1} \\ Y_{B_2} \\ Y_{B_3} \end{Bmatrix} = \begin{bmatrix} D_{T_1T_1} & D_{T_1T_2} & D_{T_1T_3} & D_{T_1B_1} & D_{T_1B_2} & D_{T_1B_3} \\ D_{T_2T_1} & D_{T_2T_2} & D_{T_2T_3} & D_{T_2B_1} & D_{T_2B_2} & D_{T_2B_3} \\ D_{T_3T_1} & D_{T_3T_2} & D_{T_3T_3} & D_{T_3B_1} & D_{T_3B_2} & D_{T_3B_3} \\ D_{B_1T_1} & D_{B_1T_2} & D_{B_1T_3} & D_{B_1B_1} & D_{B_1B_2} & D_{B_1B_3} \\ D_{B_2T_1} & D_{B_2T_2} & D_{B_2T_3} & D_{B_2B_1} & D_{B_2B_2} & D_{B_2B_3} \\ D_{B_3T_1} & D_{B_3T_2} & D_{B_3T_3} & D_{B_3B_1} & D_{B_3B_2} & D_{B_3B_3} \end{bmatrix} \begin{Bmatrix} Y_{T_1} \\ Y_{T_2} \\ Y_{T_3} \\ Y_{B_1} \\ Y_{B_2} \\ Y_{B_3} \end{Bmatrix} = \begin{Bmatrix} F_{T_1} \\ F_{T_2} \\ F_{T_3} \\ -F_{B_1} \\ -F_{B_2} \\ -F_{B_3} \end{Bmatrix}, \quad (4)$$

where $[D_s]$ is a 6×6 dynamic stiffness matrix of the primary mass–isolators substructure. The term D_{rs}, for r, $s = T_1$, T_2, T_3, B_1, B_2, B_3, represents the force at the rth d.o.f. due to a unit displacement at the sth d.o.f. of the primary mass–isolators substructure. The displacements Y_{T_1}, $Y_{T_2}$and Y_{T_3} at the mounting points between the primary mass and isolators are the three d.o.f.'s describing the motion of the primary mass. Accordingly, the original external force F_0 is split into three components F_{T_1}, F_{T_2} and F_{T_3} that are statically equivalent to F_0. These three forces are considered as excitations applied at the top of each isolator through the primary mass. The displacements of the points at which the isolators are connected to the foundation are denoted as Y_{B_1}, Y_{B_2} and Y_{B_3}. Likewise, the forces transmitted to the foundation through the three isolators are denoted as F_{B_1}, F_{B_2} and F_{B_3}. Note that the transmitted force through the ith isolator, F_{Bi}, is the superposition of the effects of the three excitation forces, i.e., $F_{Bi} = \sum_{j=1,\ \ldots\ ,3} f_{ij}$, where f_{ij} represents the transmitted force through isolator i due to the external force F_{Tj} (Fig. 6).

Similarly, the EOMs of the foundation substructure are written as

$$[\hat{D}_F]\begin{Bmatrix} Y_{B_1} \\ Y_{B_2} \\ Y_{B_3} \end{Bmatrix} = \begin{bmatrix} \hat{D}_{B_1B_1} & \hat{D}_{B_1B_2} & \hat{D}_{B_1B_3} \\ \hat{D}_{B_2B_1} & \hat{D}_{B_2B_2} & \hat{D}_{B_2B_3} \\ \hat{D}_{B_3B_1} & \hat{D}_{B_3B_2} & \hat{D}_{B_3B_3} \end{bmatrix} \begin{Bmatrix} Y_{B_1} \\ Y_{B_2} \\ Y_{B_3} \end{Bmatrix} = \begin{Bmatrix} F_{B_1} \\ F_{B_2} \\ F_{B_3} \end{Bmatrix}. \quad (5)$$

The 3×3 matrix $[\hat{D}_F]$ in Eq. (5) is the dynamic stiffness matrix of the foundation. This matrix can be obtained as the inverse of the dynamic receptance matrix of the foundation $[\hat{R}]$ [1]. That is

$$[\hat{D}_F] = [\hat{R}]^{-1} = \begin{bmatrix} \hat{R}_{B_1B_1} & \hat{R}_{B_1B_2} & \hat{R}_{B_1B_3} \\ \hat{R}_{B_2B_1} & \hat{R}_{B_2B_2} & \hat{R}_{B_2B_3} \\ \hat{R}_{B_3B_1} & \hat{R}_{B_3B_2} & \hat{R}_{B_3B_3} \end{bmatrix}^{-1}, \quad (6)$$

where the term $\hat{R}_{rs}$, for r, $s = B_1$, B_2, B_3, in the dynamic receptance matrix represents the displacement at rth point due to a unit force applied at the sth point on the foundation. The dynamic receptance matrix is obtained from the model of the foundation, which is a simply supported rectangular plate. Since the model for plate vibration is well known [12,13], it will not be presented here.

According to the continuity conditions, the displacements of the lower ends of the three isolators and the corresponding points on the foundation are equal. Therefore, the three entries of the displacement vector in Eq. (5) are the same as the last three entries of the displacement vector

in Eq. (4). Also the three forces in the force vector in Eq. (5) have same values as the last three forces in the force vector in Eq. (4).

Substituting Eq. (5) into the right side of Eq. (4), the equilibrium equations for the fully coupled system are simplified as follows:

$$\left([D_s]+\begin{bmatrix}[0] & [0]\\ [0] & [\hat{D}_F]\end{bmatrix}\right)\begin{Bmatrix} Y_{T_1}\\ Y_{T_2}\\ Y_{T_3}\\ Y_{B_1}\\ Y_{B_2}\\ Y_{B_3}\end{Bmatrix}=\begin{Bmatrix} F_{T_1}\\ F_{T_2}\\ F_{T_3}\\ 0\\ 0\\ 0\end{Bmatrix}, \tag{7}$$

where [0] denotes a 3×3 zero matrix.

Furthermore, this 3d.o.f. (in terms of the motion of the primary mass) model can be easily reduced to a s.d.o.f. model by constraining the motion of the primary mass. For instance, Eq. (7) will be simplified to Eq. (8) if the system satisfies the following two constraints: (1) the primary mass is permitted to move only in the y-direction (this happens if the rotational inertia of the primary mass is infinite); and (2) the three parallel-mounted isolators are combined into one equivalent isolator with static stiffness equal to the sum of the stiffness of the three isolators, and this equivalent isolator is connected at the center of gravity of the primary mass.

$$\left([D_s]+\begin{bmatrix}0 & 0\\ 0 & \hat{D}_F\end{bmatrix}\right)\begin{Bmatrix} Y_{T_1}\\ Y_{B_1}\end{Bmatrix}=\begin{Bmatrix} F_{T_1}\\ 0\end{Bmatrix}. \tag{8}$$

The symbols in Eq. (8) represent the same variables as in the 3d.o.f. system except that $[D_s]$ is now a 2×2 matrix representing the dynamic properties of the equivalent isolator and $\hat{D}_F$ is a scalar. Eq. (8) describes a s.d.o.f. system since the primary mass has only a vertical motion, Y_{T_1}. This system is equivalent to the 3d.o.f. system as long as the translational d.o.f. of the primary mass is concerned. Therefore, it is referred to as the *equivalent s.d.o.f. model* in the rest of the paper.

2.3. Isolation performance

The isolation performance is evaluated through the force transmissibility of the isolators and the radiated sound power of the foundation. These two attributes can be derived after obtaining the unknown displacements at the ends of each isolator. Specifically, the unknown displacements are calculated using Eq. (7), for the 3d.o.f. system, or Eq. (8), for the s.d.o.f. system. The transmitted force F_{Bi} through the ith isolator can then be evaluated by substituting the corresponding displacements into the isolator model in Eq. (1) where force F_2 in Eq. (1) represents the transmitted force, F_{Bi}. The force transmissibility is easy to calculate after knowing F_{Bi}. Furthermore, the velocity response of the foundation (plate) and the radiated sound power can also be calculated since F_{Bi} is assumed to be the only excitation to the foundation.

2.3.1. Force transmissibility

In Fig. 6, because the three isolators are coupled by the primary mass, each external force F_{Tj} will result in three transmitted forces, f_{ij}, where $i=1, 2, 3$, through the three isolators. As the result, the transmitted force at the bottom of each isolator has three components corresponding to each of the three input forces F_{Tj}, where $j=1, 2, 3$. The force transmissibility of isolator i is defined as the amplitude of the summation of these three transmitted force components at the bottom of isolator i, due to the combined action of the three input forces F_{Tj} when their amplitudes are unit. That is

$$T_i = \left| \sum_{j=1}^{3} f_{ij} \right| \quad \text{when} \quad |F_{Tj}| = 1, \tag{9a}$$

or in a more general form:

$$T_i = \left| \sum_{j=1}^{3} \frac{f_{ij}}{F_{Tj}} \right| = \left| \sum_{s=1}^{3} \frac{f_{si}}{F_{Ti}} \right|. \tag{9b}$$

The second equal mark in Eq. (9b) is because of the reciprocity principle in calculating the transmissibility between different d.o.f.s. More detail on this definition can be found in Appendix C. Eq. (9) is consistent with the definition of the *transmissibility*, which stands for the amplitude ratio of the output of a system to its input. According to Eq. (9), there are three transmissibilities for this 3d.o.f. system, one for each of the three isolators. Generally, the transmissibility of a multi-dimensional system is given by a matrix whose terms relate the input and output between any combination of two d.o.f.'s as explained in Appendix C. Actually, the definition in Eq. (9) is a combination of the column or row terms in the transmissibility matrix. It is suitable for measuring the performance of a particular isolator in a multi-dimensional system and, it allows for a direct comparison between the transmissibility of this particular isolator and its counterpart in a s.d.o.f. system. Therefore, this definition is used in this study.

2.3.2. Sound power radiated by the foundation

In Ref. [14], the radiated sound power for a plate structure embedded in an infinite baffle is given as

$$P(\omega) = \frac{\omega \rho_a}{8\pi^2} \int \int_{k_a \geqslant \sqrt{k_x^2 + k_z^2}} \frac{|v(k_x, k_z)|^2}{\sqrt{k_a^2 - k_x^2 - k_z^2}} \, \mathrm{d}k_x \, \mathrm{d}k_z, \tag{10}$$

where P is the sound power measured in watts, ρ_a is the density of the ambient medium, i.e., air, $\rho_a = 1.2\,\mathrm{kg/m^3}$, k_x and k_z are variables of integration, $k_a = \omega/c_a$ is the acoustic wavenumber measured in 1/m, ω is the frequency of the external excitation, $c_a = 343\,\mathrm{m/s}$ is the speed of sound in air, and $v(k_x, k_z)$ is the two-dimensional velocity wavenumber transform of the plate response. The velocity wavenumber transform is given as

$$v(k_x, k_z) = \int_{x=-\infty}^{x=\infty} \int_{z=-\infty}^{z=\infty} V(x, z) \mathrm{e}^{\,\mathrm{j}k_x x} \mathrm{e}^{\,\mathrm{j}k_z z} \, \mathrm{d}x \, \mathrm{d}z, \tag{11}$$

where $V(x, z)$ is the velocity response of the plate. It can be calculated by substituting the transmitted forces F_{Bi} into the simply supported plate model and expressed as a linear

combination of the plate's modes as (see Appendix D)

$$V(x,z)=\sum_{m=1}^{\infty}\sum_{n=1}^{\infty}\Phi_{mn}(x,z)q_{mn}(\omega)\mathrm{j}\omega, \tag{12}$$

where $\Phi_{mn}(x,z)$ is the modal shape and $q_{mn}(\omega)$ is the modal amplitude of the (m, n)th mode of the plate.

For the simply supported plate, Eq. (11) has a closed form given as

$$v(k_x,k_z)=\frac{2\mathrm{i}\omega\pi^2}{ab\sqrt{m_s ab}}\sum_{m=1}^{\infty}\sum_{n=1}^{\infty}q_{mn}mn\frac{[(-1)^m\mathrm{e}^{\mathrm{i}ak_x}-1][(-1)^n\mathrm{e}^{\mathrm{i}bk_z}-1]}{[k_x^2-(m\pi/a)^2][k_z^2-(n\pi/b)^2]}, \tag{13}$$

where a, b are the lateral dimensions of the plate and m_s is the mass per unit area of the plate.

After substituting Eq. (13) into Eq. (10), the acoustic power can be calculated using some numerical technique, such as the composite Simpson method.

3. Numerical results—effects of IRs on isolator performance

As mentioned in the introduction, previous studies on isolators' IRs examined the effect of IR on the force transmissibility using s.d.o.f. models [4–11]. This paper explores the importance of IRs by examining both the force transmissibility of isolators and the sound radiated from the foundation in a 3d.o.f. system. In this section, the force transmissibility and the radiated sound power are computed for the system shown in Fig. 4, which will be considered as the *reference system*.

The reference system has a primary mass $m=27.8\,\mathrm{kg}$. The moments of inertia about the x-axis and the z-axis of the primary mass are $J_{xx}=0.44$ and $J_{zz}=0.82\,\mathrm{kg\,m^2}$, respectively. An external force of amplitude F_0 is applied on the primary mass. To induce rotations of the primary mass, the force is applied off the center of gravity at $(x_F, z_F)=(0.1, 0.1)$. Fig. 7 shows a top view of the

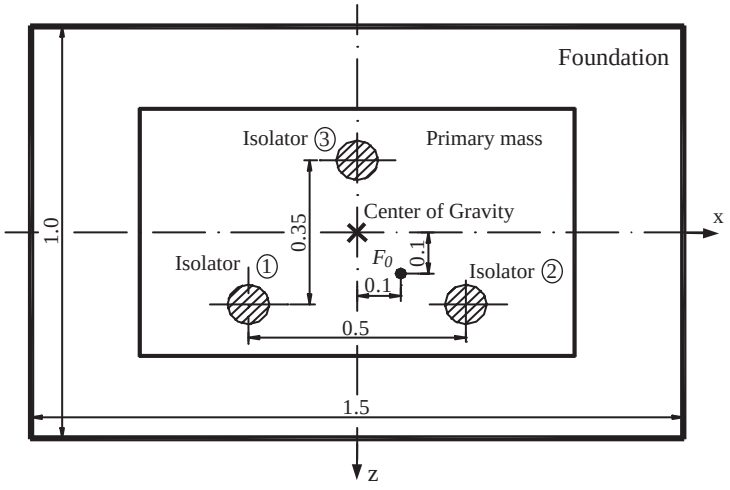

Fig. 7. Illustration for the lay out of the isolation system. (top view, dimension is measured in meter).

reference system to illustrate the positions of the external force, the primary mass, the three isolators, and the foundation. The three isolators are identical with length 0.066 m and cross-sectional area 0.00123 m^2. The isolators are made of viscoelastic material with density 1103 kg/m^3, Young's modulus 20 MPa, and loss factor 0.1. The foundation is a $1.5 \times 1 \times 0.02\,m^3$ rectangular steel plate (the long side is parallel to the x-axis) with simply supported boundary conditions. The modulus of elasticity of the foundation is 2×10^5 MPa, the density is 7800 kg/m^3, the loss factor is 0.01, and the Poisson ratio is 0.28. The above system parameters were selected on the basis of information about practical systems. For example, the primary mass represents a small car engine. The selection of the isolator parameters was based on both the properties of a commercial rubber mount manufactured by Lord Corporation and the values presented in the bibliography [4,9]. The parameters of the foundation were chosen in such a way that it simulates a typical flexible base, such as the body of a car.

In the following figures, the force transmissibility T is plotted in decibels,

$$T_d = 20 \log_{10}(T) \text{ (dB)} \tag{14}$$

and the radiated sound power is A-weighted as

$$L_{P,A} = 10\log(P/10^{-12}) + L_A \quad (\text{dBA} - \text{Ref. } 10^{-12} \text{ W}), \tag{15}$$

where L_A is the A–weighting function [15].

3.1. Effect of the IRs on the force transmissibility

According to the traditional s.d.o.f. model with a massless isolator shown in Fig. 1(a), the force transmissibility of the system will be attenuated at a rate of 12 dB per octave for frequencies well above the system natural frequency [4,5]. However, this section will show that the attenuation rate of a practical isolator is considerably lower than 12 dB per octave due to the internal dynamics of the isolator.

Fig. 8 shows the three force transmissibility curves for isolators 1, 2 and 3 in the reference system as a function of frequency. As it can be seen in Fig. 7, the positions of isolators 1 and 2 are symmetric about the z-axis. Therefore, the transmissibility curves for isolators 1 and 2 are identical. From these transmissibility curves, it is easy to identify the resonant frequencies of the reference system. These resonances correspond to the dynamics of the primary mass (i.e., system resonances), the modes of the foundation, and the IRs of the isolators. Some of the resonant frequencies of the system are listed in Table 1. The first three lowest frequencies are system resonances corresponding to one translational and two rotational d.o.f.'s of the primary mass. The resonance at 72 Hz corresponds to the first mode of the foundation ((1,1) mode). It is observed that the foundation's first mode is very significant compared with other modes. This is because the three transmitted forces through the isolators are in phase at this mode. However, it is difficult to distinguish the foundation's resonances of higher order. This is because the foundation's resonances at high frequencies have little effect on the transmissibility of the system as long as the foundation is reasonably stiff, which will be shown later in Section 3.3. The three evident resonances of the reference system at frequencies above 1000 Hz correspond to the isolators' IRs. For comparison, the transmissibility predicted from the massless model of isolator 1

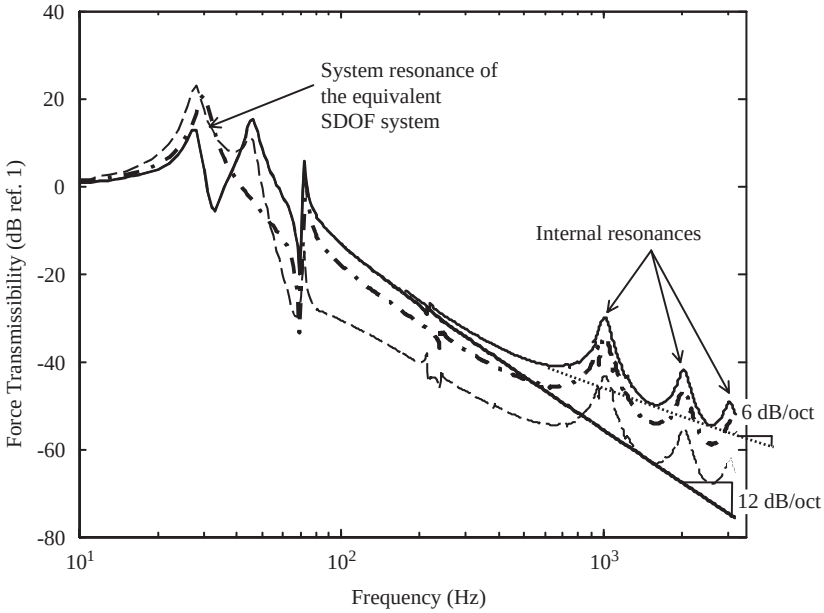

Fig. 8. Theoretical curve of transmissibility versus frequency for the reference and equivalent s.d.o.f. systems: ——, isolators 1 and 2; – – –, isolator 3; ——, isolator 1-massless; —·—, equivalent s.d.o.f.

Table 1
Resonant frequencies for the reference system

Mode		Frequency (Hz)	Note
System resonances of primary mass	1	31.2	Translation in y direction
	2	42.8	Rotation about z-axis
	3	52.4	Rotation about x-axis
Foundation's resonances	1	72.0	(1,1) mode
	2	133.3	(2,1) mode
	3	214.4	(1,2) mode
Isolators' internal resonances	1	1016.7	1st IR
	2	2033.4	2nd IR
	3	3035.8	3rd IR

and the transmissibility predicted from the equivalent s.d.o.f. model are also shown in the same figure.

Two main conclusions can be drawn from Fig. 8. First, comparing the curves for isolator 1 predicted from two models that consider and neglect the isolator mass, respectively, it is seen that the force transmissibility of the realistic isolator can be 20–30 dB higher at IR frequencies than that of the ideal massless isolator. For the case shown in the figure, the transmissibility for the portion of the curves (the valleys) between the IR peaks decreases at about 6 dB instead of 12 dB per octave [4], which indicates that the traditional isolation model with massless isolators significantly over-estimates the performance of realistic isolators at high frequencies where the IRs

occur. It should be mentioned that the asymptotic rate of decrease of the transmissibility is approximately equal to 6 dB only for small values of the loss factor, e.g., for $\eta < 0.2$.

Second, it is also interesting to compare the transmissibilities of isolators 1, 2 and 3 in the reference system to the transmissibility of the isolator in the equivalent s.d.o.f. system. It is observed that the transmissibility for one or more isolators in the reference system can be either higher or lower than the transmissibility for the s.d.o.f. system. For instance, the transmissibility of isolator 1 is 5 dB higher than that of the s.d.o.f. system at the IR frequencies. Generally, the transmissibility curve starts decreasing at a rate that depends primarily on the isolator internal damping after the highest system resonance. Therefore, when the highest resonant frequency of the primary system increases, the value of the transmissibility at the IRs increases. Since the highest resonant frequency of the reference 3d.o.f. system is higher than the resonant frequency of the equivalent s.d.o.f. system, the values of the transmissibility at the IRs of the 3d.o.f. are larger than their counterparts of the s.d.o.f. system (Fig. 8). This observation indicates that the IR problem in the multi-d.o.f. system can be more important than the s.d.o.f. model predicts. The IRs can lead to significant deterioration of the performance of one or more isolators in a multi-d.o.f. system but the s.d.o.f. model might fail to show this deterioration. It is recommended that the importance of the IRs in a practical system, for example the engine mount system of vehicles, should be assessed using a multi-d.o.f. model.

The effects of the IRs on the force transmissibility are shown in Fig. 8 for a particular set of values of their parameters. In order to evaluate the importance of the IRs in practical isolators, it is necessary to investigate how the isolator parameters affect the IRs and furthermore affect the isolator performance. It is found that the IRs, their frequencies and amplitudes, are significantly affected by three fundamental parameters: (1) the mass ratio (μ), which is defined as the primary mass to the total mass of isolators, (2) Young's modulus (E), and (3) the loss factor (η) of the isolator material.

Fig. 9 shows the transmissibility of isolator 1 in the reference system for various loss factors and mass ratios. Two values of mass ratio are considered: $\mu = 50$ and 500. For each mass ratio, the transmissibility is shown for values of the loss factor varying from 0.1 to 0.3. For comparison purpose, the transmissibility of the massless isolator for $\mu = 500$ is also shown. The resonances below 100 Hz correspond to the system resonances and the first mode of the foundation. There are two groups of system resonances—one, with higher amplitudes, is for $\mu = 50$ and the other is for $\mu = 500$. In the frequency range where the IRs are located, it is observed that the effects of the IRs become less important as μ increases because the transmissibility decreases with the mass ratio increasing. From this point of view, therefore, it is desirable for a practical isolation system to have a mass ratio as large as possible. However, no matter what the mass ratio is, the transmissibility of the realistic isolator is always 20–30 dB higher compared with the ideal massless isolator for the same system. That is, for any given mass ratio, the IRs are responsible for an additional 20–30 dB degradation of the isolator performance at some frequencies.

The advantage of high damping is also illustrated in Fig. 9. Increasing damping decreases the transmissibility at the frequency range where the resonances appear. The asymptotic decrease of the valleys between the IR peaks becomes sharper with increasing damping. It is observed that, when the material loss factor reaches 0.3, the IRs are effectively damped while the transmissibility at other frequencies decreases only slightly instead of increasing. The model that accounts for the IRs leads to opposite conclusions about the effect of damping than the traditional massless model

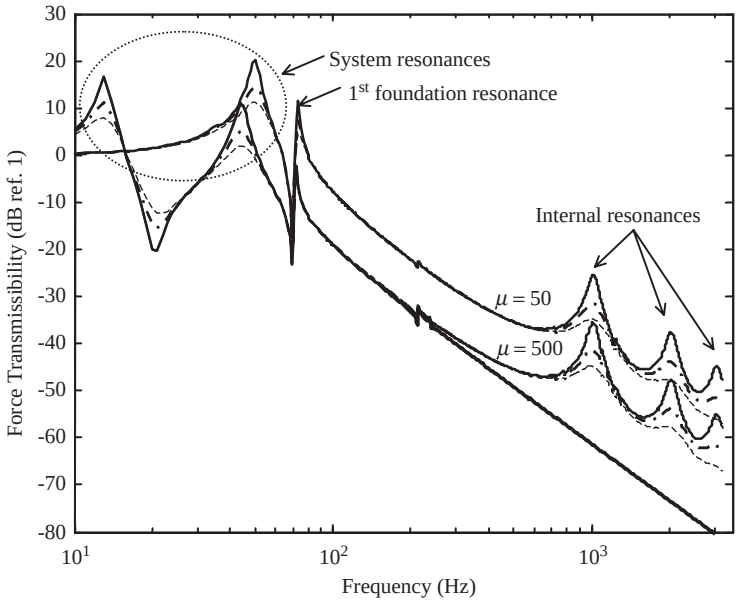

Fig. 9. Effect of mass ratio and of loss factor on transmissibility: ——, $\eta = 0.1$; —·—, $\eta = 0.2$; – – –, $\eta = 0.3$; ——, $\eta = 0.1$, massless isolator.

(Fig. 1), which predicts that higher damping can increase the transmissibility. This discrepancy is due to the different ways of representing the material damping in the models in Figs. 1 and 9 and not the difference in the number of degrees of freedom. The lumped parameter model presented in the introduction uses a constant viscous damping ratio, while the model in this paper uses a constant loss factor to characterize the isolator damping. In practical applications, the internal damping of isolator materials generally is better represented by a constant loss factor than by a constant damping ratio, particularly at high frequencies [8]. Because of the advantage of high damping, some previous researchers concluded that the IRs problem is not important since IRs can be effectively attenuated by simply increasing the damping of the isolator materials [5,11]. However, this conclusion is only correct in theory. In practice, typical highly damped elastomers exhibit poor returnability and greater drift than elastomers with medium and low damping levels [9,16]. These drawbacks limit the values of the loss factor in practical isolators. For rubber-like materials, most practical isolators have a loss factor between 0.05 and 0.2 [9]. The loss factor is less than 0.05 for metal materials [17,18]. Given these ranges for the loss factor, and the observations from Fig. 9, we can conclude that the IRs are important.

It can also be observed from Fig. 9 that neither the mass ratio nor the loss factor has appreciable influence on the IR frequencies. The IR frequencies mainly depend on Young's modulus for a given isolator.

Fig. 10 shows the force transmissibility of isolator 1 in the reference system for values of Young's modulus in the range from 10 to 30 MPa. Note that Young's modulus for natural and neoprene rubber compounds ranges from 2 to 50 MPa [9]. The mass ratio and loss factor used in Fig. 10 are constant and equal to 103 and 0.1, respectively. It is observed that when the modulus decreases, the IR frequencies decrease. Therefore, more IRs will appear below a given frequency

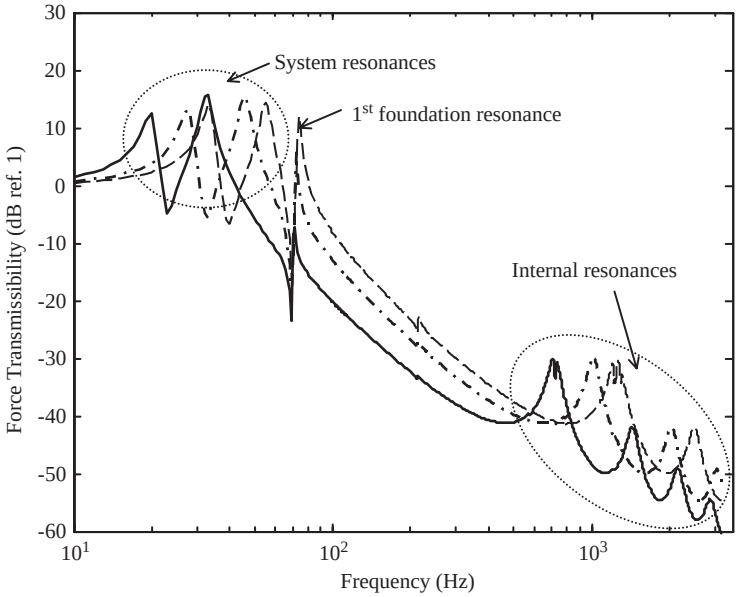

Fig. 10. Effect of Young's modulus on the force transmissibility (the 1st IR for the cases of $E=10$ and 30 MPa is coupled with one of the foundation's modes) ——, $E=10$ MPa; —·—, $E=20$ MPa; – – – –, $E=30$ MPa.

(e.g., 3000 Hz) when the value of the modulus is reduced. Young's modulus affects the transmissibility level too. Since the isolator stiffness is directly related to Young's modulus, all other parameters being equal, a smaller Young's modulus indicates a softer isolator, and lower system resonance frequencies. The traditional vibration model, which neglects IR, indicates that lowering the system natural frequency can decrease the transmissibility at high frequencies. However, this conclusion could be misleading in real-life applications where the IRs occur. The following example (based on results presented in Fig. 10) shows that, if the IRs are considered, lowering the system natural frequency by decreasing Young's modulus is not always an effective practice for improving the isolator performance at high frequencies.

Consider a system with an isolator with Young's modulus of 30 MPa. This system is subjected to a disturbance with energy in the range from 200 to 1500 Hz. If a designer finds that the isolation performance around 1400 Hz is unsatisfactory because of the first IR, and the designer is not aware of the IRs of the isolators, the designer is likely to opt for a softer isolator, for example one with modulus 20 MPa. However, although this new design will improve the isolation at around 1400 Hz as well as some other frequencies, the designer will find a new resonance appearing at 1000 Hz with almost the same amplitude as the resonance, which was originally at 1400 Hz. The reason is that switching to a softer isolator does not attenuate the original IR—it shifts the IR to lower frequencies. For instance, in the previous example, when the isolator modulus is reduced from 30 to 20 MPa, the first IR frequency is consequently shifted from 1400 to 1000 Hz, but the amplitudes at the first IR frequency for both isolators are almost the same at about –30 dB. This example reveals that if the IRs are not attenuated, decreasing or increasing the modulus of the isolator cannot improve the isolator performance.

It is also observed in Fig. 10 that there is a notch at the peak of the first IR for $E=10$ and 30 MPa. This phenomenon is due to the coupling effects between the IR and the foundation's

resonance. A notch will appear when the IR frequency coincides with one of the resonance frequencies of the foundation. The coupling effects between the IR and the foundation resonance will be discussed in Section 3.3.

3.2. Effect of the internal resonances on the radiated sound power

Force transmissibility has been widely used as a metric for the isolator performance. However, this metric does not indicate the isolator performance in terms of noise reduction. Because practical supporting structures are flexible, they will radiate noise under the excitation of the transmitted forces through isolators. Therefore, the radiated sound power should be another important measure of the isolator performance. To the best of the authors' knowledge, no publication discusses the IR problem in terms of the radiated noise.

In Fig. 11(a), the sound power radiated by the foundation of the reference system predicted by a model using isolators with inertia is compared to the power predicted by a model of the same system using massless isolators. The force transmissibility for isolator 1 is also plotted in Fig. 11(b) as a reference. For completeness, the figure is generated by assuming that the external disturbance F_0 has constant spectral density from 1 to 3000 Hz. However, in practice, the disturbance in the low frequency range (e.g., <100 Hz) including the system resonant frequencies is very small. This is because the isolation systems are designed in such a way that the excitation frequencies occur in the isolation region, i.e., at frequencies higher than system resonances (Fig. 2). Thus, for the reference system whose system resonances are all below 100 Hz, it is reasonable to assume that the excitation has little energy in frequencies below 200 Hz, and use the total sound power within the frequency band from 200 to 3000 Hz to measure the isolator performance.

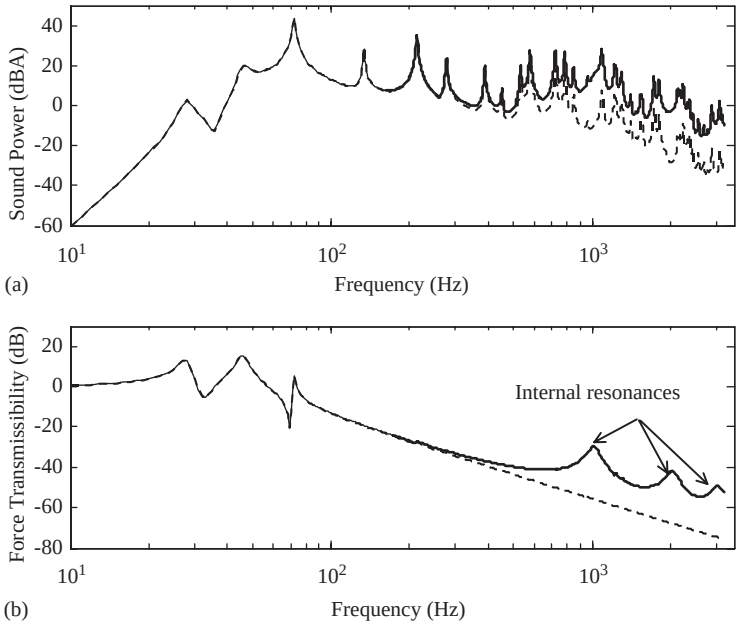

Fig. 11. (a) Radiated sound power by the foundation and (b) force transmissibility of isolator 1 of the reference system with viscoelastic isolators: ——, isolator with mass; – – – –, isolator without mass.

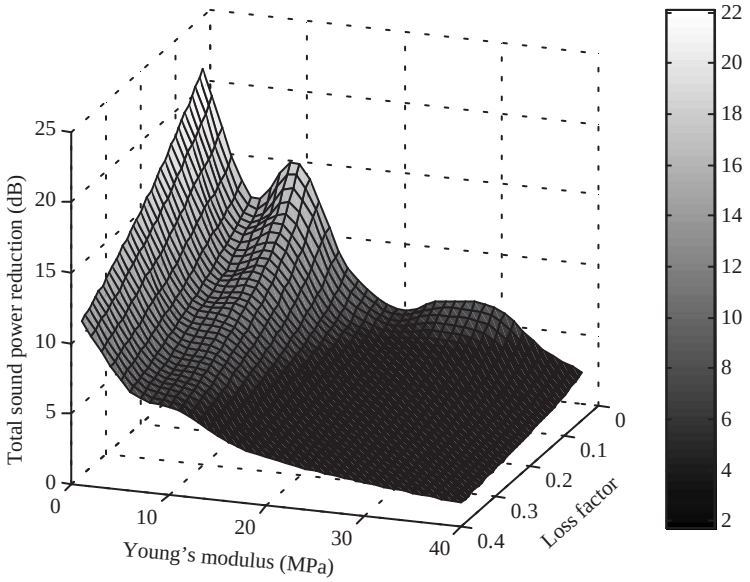

Fig. 12. Total sound power reduction in the frequency band from 200 to 3000 Hz versus Young's modulus and loss factor.

Fig. 11 shows that the radiated sound power for the realistic isolator with mass is significantly higher than the radiated sound power for the ideal, massless isolator in the range of frequencies where the IRs occur. The total sound power for the cases of realistic and ideal massless isolators are 47.6 and 41.9 dBA, respectively. This result indicates that a total sound power reduction of up to 5.7 dB can be obtained if the IRs are suppressed. The potential sound power reduction at the specific IR frequencies can be as high as 30 dB. The total sound power reduction or the sound power reduction at the specific frequency can also be interpreted as the detrimental effect of the IR on the radiated noise. These values reveal the significance of the IRs from the perspective of noise radiation.

As shown earlier, the isolator parameters affect the amplitudes and frequencies of the IRs, and consequently the level of the radiated noise. Therefore, it is useful to investigate the effect of the isolator parameters on the radiated sound power. The total sound power reduction, within the frequency range from 200 to 3000 Hz, as a function of both Young's modulus and loss factor of the isolator material, is plotted in Fig. 12. The result in Fig. 12 demonstrates the beneficial effect of high damping on the radiated noise as Fig. 9 did for the force transmissibility. It is seen that when the loss factor increases, the sound power reduction decreases. This is because the IRs are effectively attenuated by the high damping. Fig. 12 also shows that the noise reduction does not change monotonically with Young's modulus. This is due to the aggregation of the opposing effects of increasing Young's modulus on the overall response level in high frequencies and on the response at the IRs frequencies (Fig. 10). Increasing the modulus will increase the overall response level (which tends to increase the radiated noise), but it will also shift the IR frequencies towards higher frequencies. The latter effect reduces the radiated noise because the excitation is assumed to have no energy above 3000 Hz. In general, increasing Young's modulus tends to reduce noise because the IR frequencies increase faster than the amplitudes do with increasing modulus.

Fig. 12 demonstrates how much potential sound power reduction can be obtained by suppressing the IRs. It is observed that the detrimental effect of the IRs on the radiated noise, i.e., the total sound power reduction, is insignificant in the area where the loss factor is high and Young's modulus is large. However, this area is not preferred in practice because (1) high damping generally leads to large creep in viscoelastic materials and (2) large Young's modulus results in high system resonance frequencies, which degrade the isolation performance. According to the parameters of most practical isolators made of viscoelastic materials [9], the total sound power reduction ranges from 3 to 22 dB.

It should be pointed out that Fig. 12 is plotted by using values of Young's modulus and loss factor mainly for elastomers. The observations and conclusions from Fig. 12 are not valid for metal springs because, compared with elastomers, metals generally have very large modulus of elasticity and very small loss factor. Furthermore, a metal spring functions in a different way than an elastomer isolator. However, it is possible to show the effects of the IRs in the metal coil springs using the model presented in this paper. In order to conduct the analysis, the coil springs are equated to "long-rods" and the equivalent "rod-lengths" for the coil springs are calculated according to the method introduced in Ref. [7].

Fig. 13 shows the force transmissibility and radiated sound power for the reference system while replacing the viscoelastic isolators with metallic coil springs. The three coil springs are identical and have the same static stiffness as the previously used viscoelastic isolators. The loss factor used for the coil springs is 0.01, which is typical for metal material. Fig. 13(a) compares the radiated sound powers for the coil springs with and without inertia. The total sound powers for the cases of "realistic" and "ideal" massless coil springs are 65.8 and 42.1 dBA, respectively. This means that a

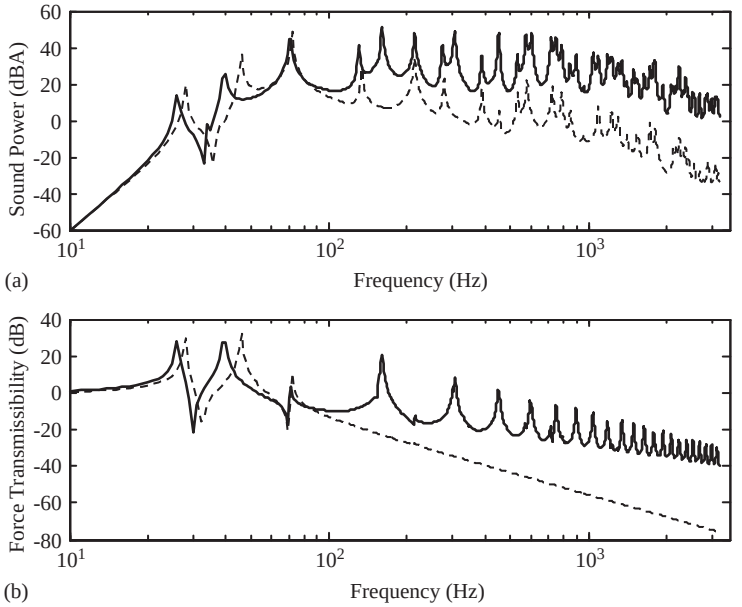

Fig. 13. (a) Radiated sound power by the foundation and (b) force transmissibility of isolator 1 of the reference system with metal coil springs: ——, isolator with mass; – – – –, isolator without mass.

total sound power reduction of 23.7 dB can be obtained by suppressing the IRs in these coil springs. The corresponding reduction in sound power for the viscoelastic isolators is only 5.7 dB. Fig. 13(b) shows that at many frequencies the transmissibility curve for the coil spring with mass, i.e., with IRs, is more than 30 dB higher than that for the coil spring without mass. The first IR of the coil spring appears at 161 Hz. Compared to the first IR of 1016.7 Hz of the viscoelastic isolators (Fig. 8), it is observed that the IRs in metal springs appear at much lower frequencies and have much higher value. These results reveal that the IRs in metal springs are very significant; they greatly increase the sound power radiated by the foundation and the force transmissibility across isolators. More detailed analysis about IRs in metal springs and their suppression can be found in Refs. [6,7].

3.3. *Influence of the foundation flexbility on the internal resonances*

In Section 3.1, it was already shown that the curve representing the force transmissibility as a function of the frequency has many resonance peaks corresponding to the foundation modes. Generally, the effect of the foundation resonances on the force transmissibility is insignificant (Figs. 9 and 10) especially at higher frequencies where the IRs usually occur [19,20]. However, changing the foundation flexibility will shift the resonant frequencies of the system. In the case where one IR frequency coincides with one of the foundation modes, the foundation acts as a dynamic vibration absorber (DVA) tuned to the IR frequency. In this case, the peak at the original IR frequency is suppressed, and two new resonance peaks appear on both sides of the original IR frequency. This effect has been shown in Fig. 10. Since the foundation flexibility does not affect significantly the characteristics of the transmissibility curve at high frequencies, the effect of this DVA is consequently slight.

Fig. 14 compares the responses of the reference system with stiff and soft foundations. The foundation stiffness is adjusted by changing the thickness while keeping all other parameters constant. Fig. 14(a) shows that the level of the radiated sound power for the soft foundation is higher than that for the stiff foundation at most frequencies. The reason is that a soft structure is more efficient for sound radiation than a stiff structure. The total sound power is 47.6 and 54.4 dBA for the stiff and soft foundations, respectively. The total sound power radiation by the soft foundation is 6.8 dB higher than that by the stiff foundation. From this perspective, increasing the foundation stiffness is a good method for reducing the noise radiation, especially when the IRs occur. On the contrary, the foundation flexibility has little influence on the force transmissibility function. As shown in Fig. 14(b), except for the obvious shifting of the resonant frequencies, the level of the transmissibility curves for soft and stiff foundations have little effect on the frequency range where the IRs occur.

3.4. *Influence of variation in the properties of isolators on the internal resonances*

The effects of changing the isolator material properties, i.e., Young's modulus and loss factor, on the IRs have been investigated in Sections 3.1 and 3.2. For simplicity, constant values of isolator properties were employed in Figs. 9 and 10. In practice, Snowdon [5,17] and Dejong et al. [21] have shown that both the dynamic modulus and the loss factor of isolator material are functions of frequency and temperature. Specifically, for room temperatures and through the

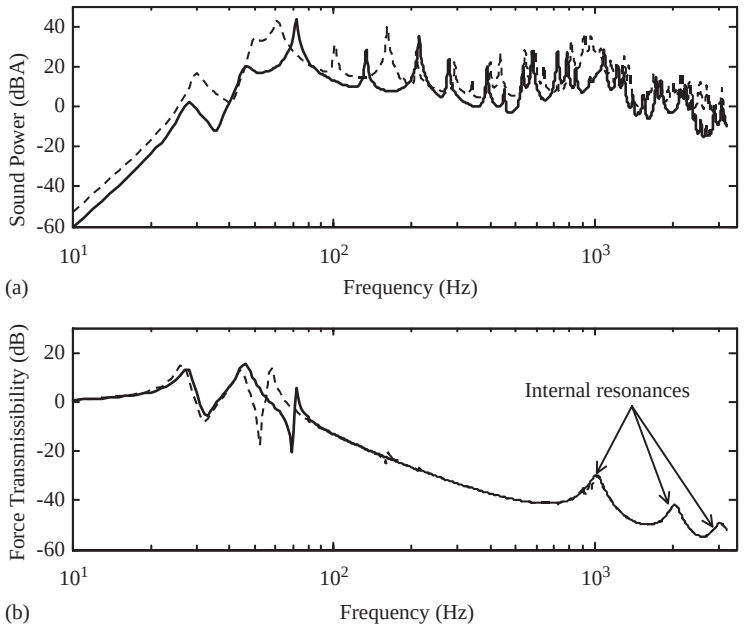

Fig. 14. (a) Radiated sound power by the foundation and (b) force transmissibility of isolator 1 of the reference system with stiff and soft foundations. ——, thickness = 20 mm (stiff); – – – –, thickness = 15 mm (soft).

range of frequencies normally of concern in vibration problems, the dynamic modulus and loss factor generally slowly increase with increasing frequency and decreases with increasing temperature.

This temperature- and frequency-dependency information can be easily synthesized with results presented in Figs. 9 and 10 to explore the significance of the IRs in practical isolators at different frequencies and temperatures. For example, it is observed from Fig. 9 that high damping helps attenuate the IR amplitudes and from Fig. 10 that increasing modulus moves IRs towards higher frequencies, which may be out of the range of interest. It is also known that practically, the modulus and damping will increase as the frequency increases. Combining all those information, it turns out that the effects of the first several IRs are dominant within the range of practical interest. Therefore, if one wants to improve the isolator performance by attenuating the IRs, one should primarily try to suppress the first several IRs.

4. Conclusions

Although researchers have been aware of the IRs in isolators since the 1950s, they did not think that they were of primary concern, particularly when viscoelastic isolators are used. This conclusion is not accurate because (1) previous researchers used a s.d.o.f. model, which may fail to reveal the importance of IRs, and (2) previous researchers did not investigate the effects of IRs on the radiated sound power.

To evaluate the importance of IRs, a system of a rigid primary mass connected to a flexible foundation through three isolators was considered in this paper. The force transmissibility and the

sound power radiated by the foundation were used as two metrics to demonstrate the significance of IRs.

Comparison of the force transmissibility of the realistic isolator model with mass and the ideal massless isolator model shows that the effects of IRs are important. The transmissibility for the isolator with mass may be 20–30 dB higher than that for the massless isolator at the IR frequencies. This result is similar to that reported by previous researchers [4–5, 8–11]. Furthermore, this paper shows that the IRs can result in a more significant deterioration of the performance of one or more isolators in a multi-d.o.f. system than previous researchers predicted using the s.d.o.f. model. Although this paper shows that the IRs in viscoelastic isolators can be attenuated using high damping of materials as previous studies stated, in real life it is impractical to build vibration isolators using materials with high damping. The loss factor in most practical viscoelastic isolators is too low to effectively suppress the IRs.

Besides evaluating the force transmissibility, one also needs to examine the radiated sound power to assess the importance of IRs. It was shown that neglecting the mass of isolators can lead to significant underestimation of the sound radiated by a foundation at frequencies around which the IRs occur. The analytical model shows that the total sound power, for the reference system, in the frequency band of 200–3000 Hz may increase 3–22 dB due to the IRs in the viscoelastic isolators.

The IRs in metal coil springs were briefly discussed in this paper. It is evident that the IR problem in metal springs is very significant from the perspective of either the force transmissibility or the radiated sound power.

Finally, it was shown that the foundation flexibility does not play an important role in the force transmissibility function of the isolator. However, the noise radiation is greatly affected by the foundation flexibility.

Acknowledgements

The study presented in this paper was partially supported by an unrestricted grant of the University Research Program of Ford Motor Company. The authors are thankful to Dr. Everett Kuo for serving as contract person between Virginia Tech, The University of Toledo and Ford Motor Company.

Appendix A. Derivation of the dyanmic stiffness matrix of the isolator

Consider the rod representing the isolator shown in Fig. 15. The rod is assumed to be thin and uniform along its length L subjected to longitudinal forces $F_1(t)$ and $F_2(t)$. The application of these forces will produce a longitudinal displacement $u(\varepsilon, t)$. The density, modulus of elasticity and cross-sectional area of the rod are denoted as ρ, E and S, respectively. To account for the damping of the rod, a complex form of the modulus of elasticity is used as follows:

$$\tilde{E} = E(1 + \mathrm{i}\eta), \tag{A.1}$$

where η is the loss factor.

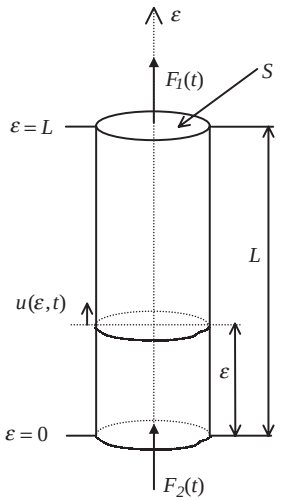

Fig. 15. Longitudinal vibration in a continuous rod.

The equation of motion for the axial vibration of this rod is given by [22]

$$\frac{\partial^2 u(\varepsilon,t)}{\partial \varepsilon^2} = \frac{1}{c^2}\frac{\partial^2 u(\varepsilon,t)}{\partial t^2}, \tag{A.2}$$

where c is the complex wave speed given as

$$c = \sqrt{\tilde{E}/\rho}. \tag{A.3}$$

The harmonic solution of the one-dimensional wave equation has the form

$$u(\varepsilon,t) = (A\mathrm{e}^{-\mathrm{i}k\varepsilon} + B\mathrm{e}^{\mathrm{i}k\varepsilon})\mathrm{e}^{\mathrm{i}\omega t}, \tag{A.4}$$

where A and B are two constants that depend on the boundary conditions, ω is the excitation angular frequency, and $k = \omega/c$ is the wavenumber.

The objective is to obtain the dynamic stiffness matrix of the isolator that relates the displacements $u(0,t)$ and $u(L,t)$ to the forces $F_1(t)$ and $F_2(t)$, i.e., a 2×2 matrix. The diagonal terms of this matrix represent the force required to induce a unit displacement on the d.o.f. where the force is applied, while the other d.o.f. is fixed. The cross terms of this matrix represent the force required to keep the d.o.f. where the force is applied fixed, while the other d.o.f. undergoes a unit displacement. Because of the reciprocity principle, the two cross terms are the same; on the other hand, the two diagonal terms are also identical due to the geometrical symmetry of the isolator. Thus, the elements in the matrix are obtained by imposing the following boundary conditions:

$$u(0,t) = 1\cdot \mathrm{e}^{\mathrm{i}\omega t}, \tag{A.5a}$$

at $\varepsilon = 0$, i.e., the displacement is assumed to be one and

$$u(L,t) = 0, \tag{A.5b}$$

at $\varepsilon = L$, i.e., the displacement vanishes at the opposite end.

The constants A and B can be computed by substituting Eq. (A.4) into Eqs. (A.5a, b) yielding

$$A = \frac{\mathrm{i}\sin(kL) + \cos(kL)}{\mathrm{i}2\sin(kL)}, \quad B = \frac{\mathrm{i}\sin(kL) - \cos(kL)}{\mathrm{i}2\sin(kL)}. \tag{A.6a, b}$$

On the other hand, the external forces at both ends of the rod should be equal to the internal forces. That is

$$-F_1(t) = -\tilde{E}S\frac{\partial u}{\partial \varepsilon}\bigg|_{\varepsilon=L}, \quad F_2(t) = -\tilde{E}S\frac{\partial u}{\partial \varepsilon}\bigg|_{\varepsilon=0}. \tag{A.7a, b}$$

Substituting Eqs. (A.6a, b) into Eqs. (A.7a, b) yields the cross terms and the diagonal terms, respectively. They are

$$D^o = kS\tilde{E}/\sin(kL), \quad D^d = kS\tilde{E}\cot(kL). \tag{A.8a, b}$$

Therefore, the dynamic stiffness matrix of the isolator is

$$\begin{Bmatrix} F_1(t) \\ F_2(t) \end{Bmatrix} = \begin{bmatrix} D^d & -D^o \\ -D^o & D^d \end{bmatrix} \begin{Bmatrix} u(L,t) \\ u(0,t) \end{Bmatrix}. \tag{A.9}$$

Appendix B. Derivation of the EOM of the primary mass–isolators substructure

The motion of the primary mass can be simply expressed with one translational d.o.f. Y_{cg} at the center of gravity, and two rotational d.o.f.'s Θ_x and Θ_z about the x- and z-axis, respectively. However, to relate motions of isolators to motions of the primary mass, it is convenient to describe the d.o.f.s of the primary mass using the three translations at the mounting points between the primary mass and isolators. As illustrated in Fig. 16, the lateral dimensions $L_x(L_z)$ of the primary mass are assumed to be much larger than the thickness t of the primary mass. Therefore, the thickness can be ignored and the three translations at the mounting points are expressed as

$$\begin{Bmatrix} Y_{T_1} \\ Y_{T_2} \\ Y_{T_3} \end{Bmatrix} = [T_c] \begin{Bmatrix} Y_{cg} \\ \Theta_x \\ \Theta_z \end{Bmatrix}, \tag{B.1}$$

where

$$[T_c] = \begin{bmatrix} 1 & -L_{1z} & L_{1x} \\ 1 & -L_{2z} & L_{2x} \\ 1 & -L_{3z} & L_{3x} \end{bmatrix}. \tag{B.2}$$

L_{rx} and L_{rz}, for $r = 1, 2, 3$, are the distances of the rth mounting point to the center of gravity in the x and z directions, respectively.

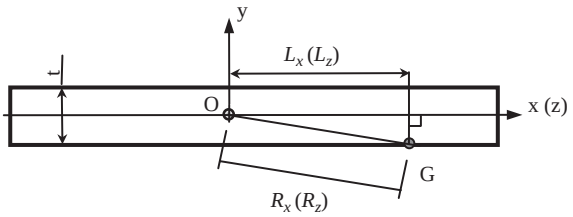

Fig. 16. Side view of the primary mass: *O*—center of gravity; *G*—mounting point between the primary mass and isolator; $L_x(L_z) >> t \Rightarrow R_x(R_z) \approx L_x(L_z)$.

The kinetic energy of the primary mass is calculated by

$$E_K = \frac{1}{2}\begin{Bmatrix} \dot{Y}_{cg} \\ \dot{\Theta}_x \\ \dot{\Theta}_z \end{Bmatrix}^{\mathrm{T}} \begin{bmatrix} m & 0 & 0 \\ 0 & J_{xx} & 0 \\ 0 & 0 & J_{zz} \end{bmatrix} \begin{Bmatrix} \dot{Y}_{cg} \\ \dot{\Theta}_x \\ \dot{\Theta}_z \end{Bmatrix}. \tag{B.3}$$

Substituting Eq. (B.1) into Eq. (B.3) gives

$$E_K = \frac{1}{2}\begin{Bmatrix} \dot{Y}_{T_1} \\ \dot{Y}_{T_2} \\ \dot{Y}_{T_3} \end{Bmatrix}^{\mathrm{T}} \left([T_c]^{-T} \begin{bmatrix} m & 0 & 0 \\ 0 & J_{xx} & 0 \\ 0 & 0 & J_{zz} \end{bmatrix} [T_c]^{-1} \right) \begin{Bmatrix} \dot{Y}_{T_1} \\ \dot{Y}_{T_2} \\ \dot{Y}_{T_3} \end{Bmatrix}. \tag{B.4}$$

Thus the mass matrix with respect to the three d.o.f.s at the mounting points is

$$[M_e] = [T_c]^{-\mathrm{T}} \begin{bmatrix} m & 0 & 0 \\ 0 & J_{xx} & 0 \\ 0 & 0 & J_{zz} \end{bmatrix} T_c^{-1}. \tag{B.5}$$

The three forces acting on the mounting points that are equivalent to the external force F_0 can be expressed by

$$\begin{Bmatrix} F_{T_1} \\ F_{T_2} \\ F_{T_3} \end{Bmatrix} = \begin{bmatrix} 1 & 1 & 1 \\ L_{1z} & L_{2z} & L_{3z} \\ L_{1x} & L_{2x} & L_{3x} \end{bmatrix}^{-1} \begin{Bmatrix} 1 \\ L_{Fz} \\ L_{Fx} \end{Bmatrix} F_0, \tag{B.6}$$

where L_{Fx} and L_{Fz} are the distances of the external force to the center of gravity in the x and z directions, respectively.

The EOM of the primary mass with respect to the three translational d.o.f. at the mounting points can be written

$$-\omega^2 [M_e] \begin{Bmatrix} Y_{T_1} \\ Y_{T_2} \\ Y_{T_3} \end{Bmatrix} = \begin{Bmatrix} F_{T_1} \\ F_{T_2} \\ F_{T_3} \end{Bmatrix} - \begin{Bmatrix} F_{e_1} \\ F_{e_2} \\ F_{e_3} \end{Bmatrix}, \tag{B.7}$$

where F_{ei} (i denotes the number of the isolator, which can be 1, 2 and 3) is the reaction force of the isolator acting on the primary mass. According to the isolator model, the reaction force of the

isolator can be computed as

$$F_{e_i} = D_i^d Y_{T_i} - D_i^0 Y_{B_i}. \tag{B.8}$$

On the other hand, the transmitted force through each isolator can be expressed as

$$-F_{B_i} = -D_i^0 Y_{T_i} + D_i^d Y_{B_i}. \tag{B.9}$$

Substituting Eq. (B.8) into Eq. (B.7) and then writing Eqs. (B.7) and (B.9) in a matrix form gives the EOM shown in Eq. (4):

$$[D_s]\begin{Bmatrix} Y_{T_1} \\ Y_{T_2} \\ Y_{T_3} \\ Y_{B_1} \\ Y_{B_2} \\ Y_{B_3} \end{Bmatrix} = \begin{bmatrix} -\omega^2[M_e] + \begin{bmatrix} D_1^d & 0 & 0 \\ 0 & D_2^d & 0 \\ 0 & 0 & D_3^d \end{bmatrix} & \begin{bmatrix} -D_1^o & 0 & 0 \\ 0 & -D_2^o & 0 \\ 0 & 0 & -D_3^o \end{bmatrix} \\ \begin{bmatrix} -D_1^o & 0 & 0 \\ 0 & -D_2^o & 0 \\ 0 & 0 & -D_3^o \end{bmatrix} & \begin{bmatrix} D_1^d & 0 & 0 \\ 0 & D_2^d & 0 \\ 0 & 0 & D_3^d \end{bmatrix} \end{bmatrix} \begin{Bmatrix} Y_{T_1} \\ Y_{T_2} \\ Y_{T_3} \\ Y_{B_1} \\ Y_{B_2} \\ Y_{B_3} \end{Bmatrix} = \begin{Bmatrix} F_{T_1} \\ F_{T_2} \\ F_{T_3} \\ -F_{B_1} \\ -F_{B_2} \\ -F_{B_3} \end{Bmatrix}. \tag{B.10}$$

Appendix C. Explanation on the definition of the force transmissibility

Theoretically, the transmissibility of a multi-dimensional system should be given as a matrix. For example, considering the system shown in Fig. 6, there are three input forces F_{Tj}, for $j=1$, 2 and 3, acting on the top of each of the three isolators; accordingly, each input force F_{Tj} results in a transmitted force f_{ij} through isolator i, for $i=1$, 2, and 3. Therefore, the transmissibility can be expressed using a 3×3 matrix as shown in Eq. (C.1). The entry at the (i, j) position of this matrix denotes the force transmitted to the plate at the bottom of isolator i due to a unit input force applied at the top of isolator j. The transmissibility matrix is written as

$$T = \begin{bmatrix} \dfrac{f_{11}}{F_{T1}} & \dfrac{f_{12}}{F_{T2}} & \dfrac{f_{13}}{F_{T3}} \\ \dfrac{f_{21}}{F_{T1}} & \dfrac{f_{22}}{F_{T2}} & \dfrac{f_{23}}{F_{T3}} \\ \dfrac{f_{31}}{F_{T1}} & \dfrac{f_{32}}{F_{T2}} & \dfrac{f_{33}}{F_{T3}} \end{bmatrix}, \tag{C.1}$$

where F_{Tj}, $j = 1, 2, 3$ are the three input forces at the points where each the three isolators are connected to the primary mass, and f_{ij} is the force at the bottom of the ith isolator due to the application of F_{Tj}, only. Due to the reciprocity principle, the matrix in Eq. (C.1) is symmetric. Note that the terms in each row correspond to the transmitted forces through a particular isolator due to the three input forces acting from the primary mass. The summation of the terms in the ith row can be considered as a metric to describe the performance of the ith isolator, which is the definition of force transmissibility in Eq. (9). Because of the symmetry of the transmissibility matrix, the row summation is equivalent to the column summation. Since the jth column terms

have the same denominator, which is the jth input force, their sum can be considered as the system transmissibility with respect to that force.

Appendix D. Velocity response of a simply supported rectangular plate under a concentrated force excitation

The displacement response of a simply supported rectangular plate under the excitation of a concentrated force is given by [12,13]

$$W(x,z,\omega)=\sum_{m=1}^{\infty}\sum_{n=1}^{\infty}\Phi_{mn}(x,z)q_{mn}(\omega), \tag{D.1}$$

where $\Phi_{mn}(x,z)$ is the mode shape and $q_{mn}(\omega)$is the modal amplitude of the (m, n) mode, which are given as

$$\Phi_{mn}(x,z)=\frac{2}{\sqrt{m_d ab}}\sin\left(\frac{m\pi x}{a}\right)\sin\left(\frac{n\pi z}{b}\right), \tag{D.2}$$

and

$$q_{mn}(\omega)=(\omega_{mn}^2-\omega^2)^{-1}\frac{2}{\sqrt{m_d ab}}\sin\left(\frac{m\pi x_f}{a}\right)\sin\left(\frac{n\pi z_f}{b}\right)F(\omega), \tag{D.3}$$

in which ω_{mn} is the (m,n) natural frequency of the simply supported plate; a, b the length and width of the plate; m_d the mass of per unit area of the plate; (x_f, z_f) the position of the external force on the plate; and $F(\omega)$: the Fourier transform of the time-dependent external force.

The velocity response of the plate is given by

$$V(x,z,\omega)=\mathrm{j}\omega W(x,z,\omega)=\sum_{m=1}^{\infty}\sum_{n=1}^{\infty}\Phi_{mn}(x,z)q_{mn}(\omega)\mathrm{j}\omega. \tag{D.4}$$

References

[1] D.J. Inman, Engineering Vibration, Prentice-Hall, Englewood Cliffs, NJ, 1994.
[2] W.T. Thomson, Theory of Vibration with Applications, Prentice-Hall, Englewood Cliffs, NJ, 1993.
[3] L.L. Beranek, Noise and Vibration Control, Wiley, New York, 1988.
[4] M. Harrison, A.O. Sykes, M. Martin, Waveeffects in isolation mounts, Journal of the Acoustical Society of America 24 (1952) 62–71.
[5] J.C. Snowdon, Vibration isolation: use and characterization, Journal of the Acoustical Society of America 66 (1979) 1245–1274.
[6] J. Lee, D.J. Thompson, Dynamic stiffness formulation, free vibration and wave motion of helical springs, Journal of Sound and Vibration 239 (2001) 297–320.
[7] G.R. Tomlinson, Vibration isolation in the low and high frequency range, Proceedings of Dynamic Vibration and Absorption Conference, Southampton, UK, Mechanical Engineering Publ. Ltd., Bury St. Edmunds, 1982, pp. 21–29.
[8] E.E. Ungar, C.W. Dietrich, High-frequency vibration isolation, Journal of Sound and Vibration 4 (1966) 224–241.
[9] A.O. Sykes, Isolation of vibration when machine and foundation are resilient and when wave effects occur in the mount, Noise Control 6 (3) (1960) 115–130.

[10] E.E. Ungar, Wave effects in viscoelastic leaf and compression spring mounts, Transactions of the American Society of Mechanical Engineers 85 (1963) 243–246.
[11] J.C. Snowdon, Vibration and Shock in Damped Mechanical Systems, Wiley, New York, 1968.
[12] L. Meirovitch, Principles and Techniques of Vibrations, Prentice-Hall, Englewood Cliffs, NJ, 1997.
[13] A. Leissa, Vibration of plates, Acoustical Society of America, Sewickley, PA, 1993.
[14] L. Cremer, M. Heckl, E.E. Ungar, Structure-borne Sound, 2nd Edition, Springer, Berlin, 1987.
[15] Acoustical Society of America ANSI S1.42–1986, American National Standard—Design Response of Weighting Networks for Acoustical Measurement.
[16] Application Note, Lord Corporation, Theory of Vibration/shock Isolators, www.lordmpd.com.
[17] J.C. Snowdon, Rubberlike materials, their internal damping and role in vibration isolation, Journal of Sound and Vibration 2 (1965) 175–193.
[18] D. Frankovich, The basics of vibration isolation using elastomeric materials, E-A-R Specialty Composites, Indianapolis, IN.
[19] Jong-Hyun Kim, Shi-Gie Jho, Hong Jae Yim, Influence of chassis flexibility on dynamic behavior of engine mount systems, SAE Transactions 942269, 1993.
[20] J.I. Soliman, M.G. Hallam, Vibration isolation between non-rigid machines and non-rigid foundations, Journal of Sound and Vibration 8 (1968) 329–351.
[21] R.G. Dejong, G.E. Ermer, C.S. Paydenkar, T.M. Remtema, High frequency dynamic properties of rubber isolation elements, Proceedings of Noise Control, Ypsilanti, MI, 1998.
[22] L.E. Kinsler, A.R. Frey, A.B. Coppens, J.V. Sanders, Fundamentals of Acoustics, 4th Edition, Wiley, New York, 2000.